Surface and guided waves in porous materials

Jan Descheemaeker, Jean-Philippe Groby, Philippe Leclaire, Walter Lauriks

10ème **C**ongrès **F**rançais d'**A**coustique

Lyon, 12-16 Avril 2010

Surface and guided waves in porous materials

Jan Descheemaeker[1], Jean-philippe Groby[2], Philippe Leclaire[3], Walter Lauriks [3]

[1] K.U. Leuven, Celestijnenlaan 200D, 3001 Heverlee

[2] ISEN, Boulevard Vauban, Lille

[3] ISAT, Nevers

The last decades, a lot of research has been done about the propagation of sound in heterogeneous and porous materials. Especially the two-phase nature of the poro-elastic material leads to interesting physical phenomena. During recent years, several measuring methods have been developeded to determine the material parameters.
However, a lot of problems aren't solved yet. Because of the visco-elastic behavior of a lot of these materials, the elastic moduli will become frequency dependent (rubberlike behavior at low frequencies and glasslike behavior at high frequencies). Experimental data about the frequency- and temperature dependence of the elastic moduli are scarce because of experimental difficulties. Some experimental and numerical results about this subject will be presented.
Porous materials still have to be studied in a lot of configurations. One of them is a porous material in an elastic cylinder. Some numerical results about the dispersion curves of the wave propagating in the system will be presented. These will be compared with some experimental results.

1 Introduction

One of the remaining problems in characterizing porous sound absorbing materials is the evaluation of the elastic parameters of the frame. Since the frame materials are often viscoelastic, the Lamé coefficients are frequency dependent. The traditional quasi-static techniques for evaluating these elastic parameters provide data for a frequency range that is relatively low (up to 500 Hz - 1 kHz). The transfer function method was used for investigating the complex modulus of a spring like [1] and rod-like specimen [2], the vibrational response of a clamped rectangular porous plate was studied in ref [3] and quasi-static measurement techniques were used to determine the frequency dependence of the elastic properties of acoustic foams [4]. Because all these methods focus on the recovery of the elastic constants only at low frequencies, new methods should be developed. Wave propagation in a porous semi-infinite half space (Rayleigh wave), in a porous plate on a rigid surface (Lamb-like waves) or in a porous plate (Lamb waves) was studied in [5, 6] and the frequency dependence of the elastic parameters was determined from these studies at a few kHz.

In this paper, this idea is explored further and the circumferential waves on a layered poroelastic cylinder is studied. Rayleigh waves were largely studied in elastic cylinders, as for example for a duraluminium cylinder [7], and an elastic cylinder with elastic coating [8]. Contrary to the Rayleigh wave in semi-infinite half space, the latter one is dispersive in circular shape configurations. Higher velocity modes excists and are called whispering gallery waves. While the Rayleigh wave propagates on the surface of the cylinder, whispering gallery waves have displacements more concentrated in the inner part of the cylinder[9]. The effect of the dispersion is particularly visible at low frequencies, the high frequency limit of the velocities being the Rayleigh velocity in a plate of the same material. The following study constitutes a first brakethrough, to our knowledge, in the analysis of Rayleigh wave in a porous cylinder.

The rationale behind this work is laboratory scale foam rising tests in a circular cup, for use by manufacturers of chemical components of plastic foams to study and develop new foam materials. Being able to monitor the elastic parameters while the material is changing from a liquid mixture to a solid foam (polymerisation) and/or to evaluate the final elastic modulus of the foam material is of considerable interest. Surface acoustic waves that propagate in an elastic foam mainly depend on the density and shear modulus of the frame, while they are mostly independent of the bulk modulus for most of these materials [6]. Following the shear modulus of the foam during its rising, when the chemicals change from a fluid mixture to a poroelastic foam is a first possible application of the method described in this paper. The evaluation of the shear modulus of the final poroelastic foam once formed is a second application. These applications hold for the density of the frame.

2 Description of the configuration

The geometrical configuration and the solicitation are assumed to be invariant with respect to the Cartesian coordinate x_3.
Figure 1 depicts a cross-sectional plane view of the configuration. The domain $\Omega^{[0]}$ is occupied by a fluid medium material $M^{[0]}$. The circular cylindrical domain $\Omega^{[2]}$ of

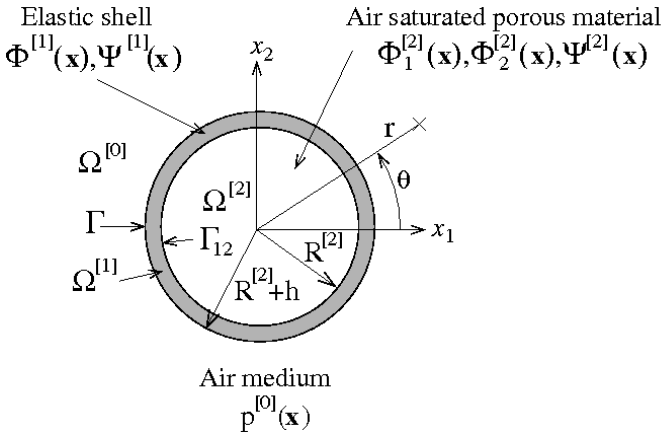

FIGURE 1 – Cross-sectional plane view of the configuration of a porous cylinder coated by an elastic shell.

radius $R^{[2]}$ is centered at the origin of the global polar coordinate system (r, O, θ) attached to the configuration and is occupied by an elastic porous material $M^{[2]}$ saturated by the fluid $M^{[0]}$. The latter domain is either in welded contact with the domain $\Omega^{[0]}$ through the interface Γ, or in welded contact with an elastic medium $M^{[1]}$, occupying the domain $\Omega^{[1]}$ of thickness h through the interface Γ_{12}. In the latter case, $\Omega^{[1]}$ is in welded contact with $\Omega^{[0]}$ through the interface Γ at $R^{[2]}+h$.

3 Rayleigh wave in a circular porous cylinder with and without elastic coating

The aim of this section is to determine the roots of the dispersion relation in order to evaluate the whispering gallery waves and Rayleigh wave velocities in a porous cylinder coated or not by an elastic shell. The problem reduces to the evaluation of the driving agent matrix, i.e. the matrix which is formed by the elements that arise when the field expressions are introduced in the boundary conditions.

3.1 Field representations and material modeling

In $\Omega^{[0]}$, the scattered pressure field can be written as :

$$p^{[0]}(\mathbf{x}) = \sum_{n\in Z} B_n \mathrm{H}_n^{(1)}\left(k^{[0]}r\right) e^{\mathrm{i}n\theta} \ . \tag{1}$$

wherein $\mathrm{H}_n^{(1)}$ is the n-th order Hankel function of first kind and B_n are the scattered coefficients by the circular cylinder.

In $\Omega^{[1]}$, the scattered scalar $\phi^{[1]}$ and vector $\psi^{[1]} = \psi^{[1]}\mathbf{i}_3$ potentials, related to the displacement $\mathbf{u}^{[1]}$ through $\mathbf{u}^{[1]} = \nabla\phi^{[1]} + \nabla\times\psi^{[1]}$ take the forms :

$$\begin{aligned}
\phi^{[1]}(\mathbf{x}) &= \sum_{n\in Z}\left[C_n \mathrm{J}_n\left(k_P^{[1]}r\right) + D_n\mathrm{H}_n^{(1)}\left(k_P^{[1]}r\right)\right] e^{\mathrm{i}n\theta} \ , \\
\psi^{[1]}(\mathbf{x}) &= \sum_{n\in Z}\left[E_n \mathrm{J}_n\left(k_S^{[1]}r\right) + F_n\mathrm{H}_n^{(1)}\left(k_S^{[1]}r\right)\right] e^{\mathrm{i}n\theta} \ ,
\end{aligned} \tag{2}$$

wherein J_n is the n-th order Bessel function.

In $\Omega^{[2]}$, the scattered scalar $\phi_1^{[2]}$ and $\phi_2^{[2]}$ and vector $\psi^{[2]} = \psi^{[2]}\mathbf{i}_3$ potentials, related to the displacement $\mathbf{u}^{[2]}$ in the solid phase through $\mathbf{u}^{[2]} = \nabla\left(\phi_1^{[2]} + \phi_2^{[2]}\right) + \nabla\times\psi^{[2]} = \nabla\phi^{[2s]} + \nabla\times\psi^{[2]}$ and in the fluid phase through $\mathbf{U}^{[2]} = \nabla\left(\mu_1\phi_1^{[2]} + \mu_2\phi_2^{[2]}\right) + \nabla\times\mu_3\psi^{[2]} = \nabla\phi^{[2f]} + \nabla\times\mu_3\psi^{[2]}$ take the forms :

$$\begin{aligned}
\phi_1^{[2]}(\mathbf{x}) &= \sum_{n\in Z} G_n \mathrm{J}_n\left(k_1^{[2]}r\right) e^{\mathrm{i}n\theta} \ , \\
\phi_2^{[2]}(\mathbf{x}) &= \sum_{n\in Z} N_n \mathrm{J}_n\left(k_2^{[2]}r\right) e^{\mathrm{i}n\theta} \ , \\
\psi^{[2]}(\mathbf{x}) &= \sum_{n\in Z} O_n \mathrm{J}_n\left(k_3^{[2]}r\right) e^{\mathrm{i}n\theta} \ .
\end{aligned} \tag{3}$$

Expressions of μ_i and $k_i^{[2]}$ (i=1, 2, 3) can be found in ref [10].

3.2 Circular porous cylinder saturated by air

Since $M^{[0]}$ is fluid and $M^{[2]}$ is a porous material, the normal total stress, pressure and normal component of the displacement should be continuous across Γ ($r = R^{[2]}$, $\forall\theta\in[0,2\pi]$, the definition of r and θ is shown in figure 1) :

$$\begin{aligned}
&\sigma_{rr}^s(R^{[2]},\theta) + \sigma_{rr}^f(R^{[2]},\theta) + p^{[0]}(R^{[2]},\theta) = 0 \ , \\
&\sigma_{r\theta}^s(R^{[2]},\theta) = 0 \ , \\
&-\frac{\sigma_{rr}^f(R^{[2]},\theta)}{\phi} - p^{[0]}(R^{[2]},\theta)) = 0 \ , \\
&u_r^{[2]}(R^{[2]},\theta) + w_r^{[2]}(R^{[2]},\theta) - U_r^{[0]}(R^{[2]},\theta) = 0 \ ,
\end{aligned} \tag{4}$$

wherein $\mathbf{w}^{[2]} = \phi\left(\mathbf{U}^{[2]} - \mathbf{u}^{[2]}\right)$ is the relative fluid displacement [11].

3.3 Circular porous cylinder coated by an elastic medium

Since $M^{[0]}$ is fluid and $M^{[1]}$ is an elastic material, the normal stress and normal component of the displacement should be continuous across Γ ($r = R^{[2]}+h$, $\forall\theta\in[0,2\pi]$) :

$$\begin{aligned}
&\sigma_{rr}^{[1]}(R^{[2]}+h,\theta) + p^{[0]}(R^{[2]}+h,\theta) = 0 \ , \\
&\sigma_{r\theta}^{[1]}(R^{[2]}+h,\theta) = 0 \ , \\
&u_r^{[1]}(R^{[2]}+h,\theta) - U_r^{[0]}(R^{[2]}+h,\theta) = 0 \ ,
\end{aligned} \tag{5}$$

Since $M^{[1]}$ is a elastic material and $M^{[2]}$ is a porous material, the normal total stress and the displacements should be continuous across Γ_{12} ($r = R^{[2]}$, $\forall\theta\in[0,2\pi]$) :

$$\begin{aligned}
&\sigma_{rr}^s(R^{[2]},\theta) + \sigma_{rr}^f(R^{[2]},\theta) - \sigma_{rr}^{[1]}(R^{[2]},\theta) = 0 \ , \\
&\sigma_{r\theta}^s(R^{[2]},\theta) - \sigma_{r\theta}^{[1]}(R^{[2]},\theta) = 0 \ , \\
&u_r^{[2]}(R^{[2]},\theta) - u_r^{[1]}(R^{[2]},\theta) = 0 \ , \\
&u_\theta^{[2]}(R^{[2]},\theta) - u_\theta^{[1]}(R^{[2]},\theta) = 0 \ , \\
&u_r^{[2]}(R^{[2]},\theta) - U_r^{[2]}(R^{[2]},\theta) = 0
\end{aligned} \tag{6}$$

Introducing the proper field and potentials expressions in Eq.(4, 5 , 6) , projecting the latter such that

$\int_0^{2\pi} \cdot \times e^{-\mathrm{i}l\theta} d\theta$ and making use of the orthogonality relation $\int_0^{2\pi} \cdot \times e^{\mathrm{i}(n-l)\theta} = 2\pi\delta_{ln}$, leads, after rearrangement, to a driving agent D.

3.4 Numerical evaluation of the roots of the dispersion curves

The determinant of D calculated as a function of the frequency f and of the order of the bessel and hankel functions n. The minima of its absolute value are then evaluated in first approximation. From couples (f_{min}, n_{min}) for which $|det(D)|$ is minimum, the phase velocity of the corresponding modes is evaluated through $2\pi f_{min} R/n_{min}$ in the case of a porous cylinder and through $2\pi f_{min}(R+h/2)(1+\frac{h}{2(R+h/2)})/n_{min}$ in the case of a porous cylinder with elastic coating [8].

The dispersion curves as calculated with the previously described algorithm were validated in the case of a duraluminium cylinder by matching the results with those found in [7]. Without dissipation, the minima of $|det(D)|$ agree with the roots of $det(D) = 0$. For porous material cylinders, the phase velocity should be complex rigurously. Nevertheless, it becomes difficult to solve this, because it imposes to use complex order Hankel and Bessel functions, in order to evaluate complex velocities of the modes [12]. The evaluation is not straightforward and largely increase the calculation time.

4 Numerical results and discussion

Contrary to the Rayleigh wave on a flat surface, the Rayleigh type wave on a cylinder exhibits geometrical dispersion, which should be distinguished from the material dispersion of the porous core.

At low frequencies, the phase velocity depends on the frequency, its high frequency limit being the Rayleigh velocity in semi-infinite half space of the material. This can clearly be noticed in figures 2 and 3. The mode with the lowest velocity values is the Rayleigh wave. The others are the whispering gallery waves. These waves arise due to the finite curvature of the surface. They are associated with the material properties of the elastic cylinder, and can be represented in a ray model as multiple reflections around the inner surface of the cylinder. These whispering gallery waves present a cut-off frequency, below which they can not propagate in the material because they are highly damped.

The porous material studied in this paper is Fireflex (Recticel, Wetteren, Belgium), whose parameters are reported in table 1 and were determined by traditional methods[13]. The radius of the ciruclar cylinder is $R^{[2]} = 75$ mm.

4.1 Numerical results for porous cylinder saturated by air

In this section the influence of the Biot parameters on the dispersion curves is studied in case of a porous cylinder saturated by air.

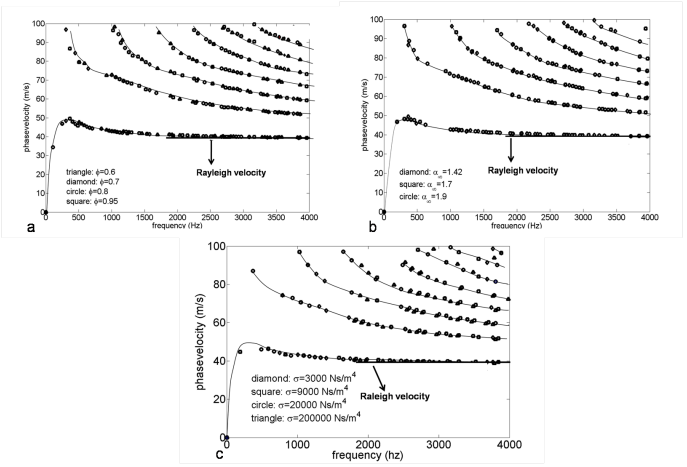

FIGURE 2 – Influence of (a) the porosity, (b) the tortuosity and (c) the flow resistivity on the dispersion curves of different modes propagating in a Fireflex cylinder of radius $R^{[2]} = 75$ mm. The other parameters are kept constant to those of Table 1.

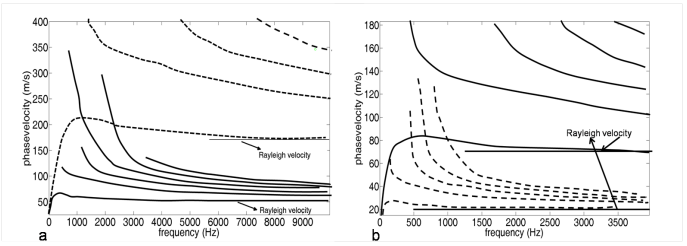

FIGURE 3 – Influence on the dispersion curves of the different modes propagating in a Fireflex cylinder of radius $R^{[2]} = 75$ mm of the shear modulus (a) : $N = 10^5$ Pa (– – –) and $N = 10^6$ Pa (—) and density (b) : ρ =30 kg.m^{-3} (– – –) and ρ =100 kg.m^{-3} (—).

For each simulation that corresponds to figure 2, one parameter is varied, while the other parameters (Biot and others, like the density) are kept constant. The dispersion curves, for the different material parameters can not be clearly distinguished, figure 2. Apparently the porosity, tortuosity and flow resistivity have a small influence on the Rayleigh wave velocity, whose high frequency limit is 40 m.s^{-1}. The same can be said for the influence on the velocity of the whispering gallery waves. This lake of sensitivity can be expected because the Rayleigh velocity is mainly determined by the density and elasticity of the material, the Rayleigh wave mainly propagating in the skeleton.

This can be seen in figures 3 (a) and (b) where the shear modulus and density of the porous cylinder were varied while all other parameters were kept constant. When the shear modulus increases or the density decreases, the phase velocity of the modes increases.

This method can also not be used to characterize the acoustical and structural parameters, but it can be used to determine the elastic properties of the foam. Since there is a clear difference in the dispersion curves for foams with different shear modulus, it will be possible to follow the shear modulus during the foam formulation with this technique.

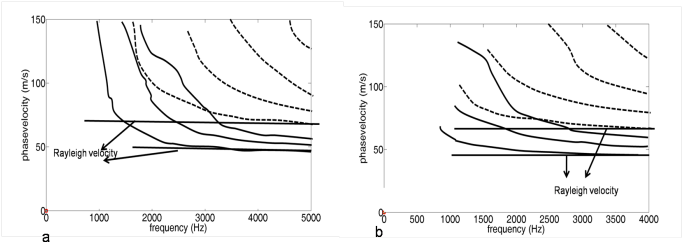

FIGURE 4 – Phase velocity of the modes in a porous cylinder, with a shear modulus of 5 10^4 Pa (– – –) and 10^5 Pa (—), coated with (a) a plexiglass shell or (b) a steel shell.

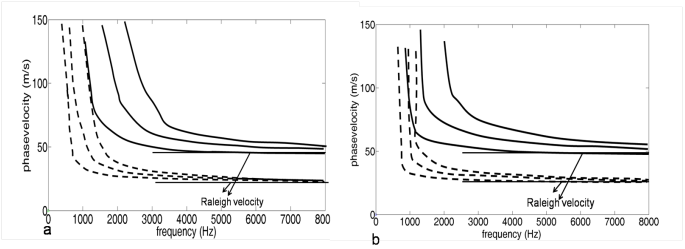

FIGURE 5 – Phase velocity of the modes of a porous cylinder, with density of 30 kg.m^{-3} (– – –) and 100 kg.m^{-3} (—), coated with (a) a plexiglass shell and (b) a steel shell.

4.2 Numerical simulations for a porous cylinder with an elastic coating

Due to the presence of the elastic coating, it can be expected that the sensitivity of the dispersion curves to the value of the elastic modulus of the porous core depends on the coating thickness and properties. If the coating thickness is small when compared with the wavelength or better when compared with the penetration depth of the quasi-Rayleigh wave, the quasi-Rayleigh wave should depend on the porous properties. In other words, it means that if the configuration is sollicited at a sufficiently low frequency, the quasi-Rayleigh wave should depend on the porous material properties. Various coating thicknesses and coating materials are also tested in order to determine the combination from which the maximum of information on the properties of the porous foam can be expected.

Simulations were performed for a porous cylinder of Fireflex with a shear modulus of 5 10^4 Pa and 10^5 Pa and an elastic coating of plexiglass ($C_P^{[1]} = C_S^{[1]} =$ 1120 m.s^{-1} and $\rho^{[1]} = 1180$ kg.m^{-3}) and steel ($C_P^{[1]} = C_S^{[1]} = 3230$ m.s^{-1} and $\rho^{[1]} = 7700$ kg.m^{-3}) of thickness $h = 1$ mm, figure 4. When the shear modulus of the porous material increases, the phase velocities increases. For both steel and plexiglass coating, the waves velocities are clearly different between a porous material with a shear modulus of 5 10^4 Pa and 10^5 Pa. Thus that both a steel and plexiglass coating can be used to determine the shear modulus of the porous cylinder. It also follows that the shear modulus can be determined during the formation process of the foam.

The same has been done to investigate the sensitivity of the dispersion curves to the density of the porous cylinder. Simulations were performed for a porous cylinder with densities of 30 and 100 kg.m^{-3} with both a plexiglass and steel coating, (figure 5). The modes can be clearly distinguished for both the steel and plexiglass coating between density of 30 kg.m^{-3} and 100 kg.m^{-3} porous material.

4.3 Experimental methods

Two experimental methods are used to determine the dispersion curves of the modes propagating in the system.
The experimental principle consists in generating circumferential waves on the surface of a porous sample with the help of a shaker and in detecting the normal

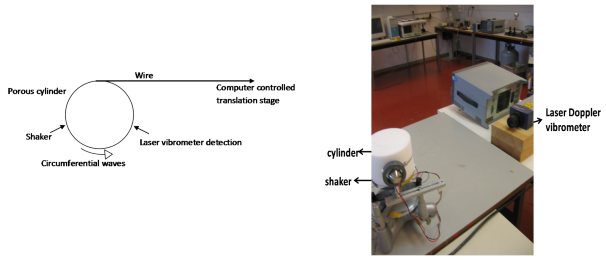

FIGURE 6 – Measurement set up for the determination of the phase velocity of the modes.

component of the surface velocity with a Laser vibrometer (Polytec OFV-505), after the waves have travelled some distance. A cylindrical sample of 15 cm diameter is placed on a circular rotating plate (Figure 6), the axis of the cylinder coinciding with the one of the disk. The shaker is attached to the sample so that there is no relative motion between them. The shaker used is fairly small and light and can provide signals at frequencies up to 10 kHz. The distance between the source and the detection point can be varied by rotating the set shaker/sample while the laser beam is not moved. The rotation angle of the sample can be controlled with precision with the help of wire connecting the periphery of the circular disk to a computer controlled translation stage.

A narrow strip of steel (0.5 x 3 cm) glued to the shaker is used as line source to generate circumferential waves on the cylindrical sample (the strip is parallel to the axis of the cylinder). The surface velocity is measured with a laser beam coming from a laser Doppler vibrometer. A narrow strip of reflecting tape of negligible thickness is glued on the surface of the cylinder so that the circumferential waves can be detected at different positions on the surface.

Two different ways of excitation were used. In a first excitation method, sine burstwaves are used to excite the sample. The phase velocity is obtained from the slope of the curve which is obtained by plotting the distances as a function of the arrival times. A more detailed description of this method can be found in [5, 6].
In a second excitation method, a pulse is used to excite the sample. The technique consists in recording the time signals on a digital oscilloscope at regular intervals of distance. It is therefore possible to create a two dimensional array s(x,t) providing values of the signal at different times and distances. If the resolution in time

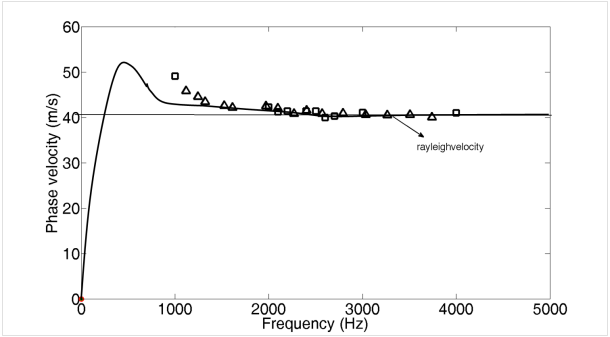

FIGURE 7 – Experimental (triangle : pulse excitation, square : burst excitation) and theoretical (full line) dispersion curves for a porous cylinder of Fireflex.

and in space are appropriately chosen, the dispersion curves are directly obtained by taking the double time and space Fourier Transform, thus providing a function $S(k, \omega)$. The phase velocities of the modes can be determined by $v = \omega k$. The line is a mode which can be detected.

4.4 Experimental results

The experimental (triangle : pulse excitation, square : burst excitation) and theoretical (circle) dispersion curves for a porous cylinder of Fireflex (the properties of the material are given in Table 1) with a radius of 7.5 cm are plotted in figure 7. With both experimental methods, the mode with lowest phase velocity is observed for frequencies lower than 4000 Hz. In the asymptotic high frequency regime, the phase velocity of this mode equal the Rayleigh velocity of the material. This is the Rayleigh mode. Both the theory and experiments provide a Rayleigh velocity close to 40 m.s^{-1}. The shear modulus used in the theoretical simulation was determined by measuring the Rayleigh velocity on a flat surface [14].

For higher frequencies, the burst method cannot be used due to the proximity of other modes resulting in mixing of the modes in the time signals.

5 Conclusions

A theoretical model was developed for the configuration of a porous cylinder with and without elastic coating. The influence of the Biot paramters of the porous material on the dispersion curves of the modes was studied. Structural parameters like the tortuosity, flow resistivity and porosity do not influence the phase velocity in a significant way and this influence will not be detectable experimentally. The shear modulus and density on the other hand influence the phase velocities of the modes in an important way. Simulations were made with a porous cylinder of Fireflex and an elastic coating of steel and plexiglas. In both cases, when the shear modulus of the porous cylinder was varied, the change of the dispersion curves could clearly be seen. This means that this method can be used to determine the shear modulus and the shear modulus can be followed during the rising of the foam. The same simulations were made for the density of the porous cylinder. There could also be concluded that the density can be followed during the rising of the foam.

Two measurement techniques were used to determine the phase velocities of the modes propagating in the case of a Fireflex porous cylinder without coating, using respectively burst excitation and pulse excitation. The first method can not be used for frequencies higher than 4000 Hz due to the proximity of other modes resulting in mixing of the modes in the time signals. Measurements were done for a porous cylinder of Fireflex without coating. A good agreement with numerical simulations was found. Both the experiment and numerical simulations resulted in a Rayleigh velocity around 40 m.s^{-1}.

Références

[1] T. Pritz. Transfer function method for investigating the complex modulus of acoustic materials : spring-like method. *J. Sound & Vib.*, 72 :317–341, 1980.

[2] T. Pritz. Transfer function method for investigating the complex modulus of acoustic materials : rod-like method. *J. Sound & Vib.*, 81 :359–376, 1982.

[3] P. Leclaire. The vibrational response of a clamped rectangular porous plate. *J. Sound & Vib.*, 247 :19–31, 2001.

[4] M. Etchessahar, S. Sahraoui, L. Benyahia, and J.F. Tassin. Frequency depencence of elastic properties of acoustic foams. *J. Acoust. Soc. Am.*, 117 :1114–1121, 2005.

[5] L. Boeckx, P. Leclaire, P. Khurana, C. Glorieux, W. Lauriks, and J.F. Allard. Investigation of the phase velocities of guided acoustic waves in soft porous layers. *J. Acoust. Soc. Am.*, 117 :545–554, 2005.

[6] L. Boeckx, P. Leclaire, P. Khurana, C. Glorieux, W. Lauriks, and J.F. Allard. Guided elastic waves in porous materials saturated by air under lamb conditions. *J. Appl. Phys.*, 97 :094911, 2005.

[7] D. Clorennec and D. Royer. Analysis of surface acoustic wave propagation on a cylinder using laser ultrasonics. *Appl. Phys. Let.*, 82 :4608–4610, 2003.

[8] U. Kawald, C. Desmet, W. Lauriks, C. Glorieux, and J. Thoen. Investigation of the dispersion relations of surface acoustic waves propagating on a layered cylinder. *J. Acoust. Soc. Am.*, 99 :926–930, 1996.

[9] D. Royer and D. Clorennec. Theoretical and experimental investigation of rayleigh waves on cylindrical and spherical surfaces. *L.U. 2008 Montreal*, 2008.

[10] M.A. Biot and D.G. Willis. The elastic coeffecients of the theory of consolidation. *J. Appl. Mechanics*, 24 :594–601, 1957.

[11] T. Bourbie, O. Coussy, and B. Zinszner. *Acoustics of Porous media.* Technip, 1987.

[12] I.S. Gradstein and I.H Ryshik. *Tables of Series, Products and Integrals.* S.l. : Academic Press, 1965.

[13] J.-F. Allard and N. Atalla. *Propagation of Sound in Porous Media : Modelling Sound Absorbing Materials*. Wiley, 2009.

[14] J.F. Allard, G. Jansens, G. Vermeir, and W. Walter. Frame borne surface waves in air-saturated porous media. *J. Acoust. Soc. Am.*, 111 :690–696, 2001.

TABLE 1 – Sample parameters of the porous samples studied in this paper, determined by the methods described in[13].

	Fireflex
$R^{[2]}$ (mm)	75
ρ(kg.m^{-3})	32
ϕ	0.95
α_∞	1.42
σ (Ns.m^{-4})	8900
Λ (μm)	180
Λ' (μm)	360
N (Pa)	56000
E (Pa)	140000